

## Nonlinear FVDs for Seismic Resilience of Irregular RC Buildings

BED PRAKASH GUPTA<sup>1\*</sup>

**ABSTRACT.** Passive energy dissipation systems, particularly fluid viscous dampers (FVDs), offer a promising alternative by enhancing damping ratios without significantly altering structural stiffness. Despite their global success, FVDs remain underutilized in Nepal due to limited studies and the absence of specific provisions in the Nepal Building Code (NBC 105:2020). This study addresses this gap by evaluating the efficacy of FVDs in enhancing the seismic performance of a 10-storey representative building with setback, exhibiting vertical irregularities using performance-based design principles in SAP2000 v20. Nonlinear behavior is modeled using a lumped plasticity approach, with user-defined moments M3 hinges for beam and auto hinges PM2M3 for columns as per ASCE 41-13. Pushover analysis determines the capacity curve, which is matched with NBC 105:2020 elastic spectrum to identify performance point and ensure compliance with the Immediate Occupancy (IO) performance level. FVDs are modeled as two-noded nonlinear link elements and strategically placed at stories with maximum inter-storey drift. Nonlinear time history analysis (NLTHA), employing the direct integration and spectrum-compatible ground motion records for Type D soil (DBE, 10% probability of exceedance in 50 years), evaluates maximum storey displacements and hinge states. Comparative results between damped and undamped models are analyzed to quantify performance improvements. The results demonstrate that FVDs significantly reduce displacements and maintain hinge state within the IO performance level, offering practical and effective strategy for enhancing seismic resilience.

**Keywords:** Fluid viscous damper (FVDs), Plastic hinges, Push over analysis, Roof displacement, Time history analysis.

---

<sup>1</sup>Department of Civil Engineering, Everest Engineering College, Sanepa, Lalitpur, Nepal  
E-mail: bedp.gupta@eemc.edu.np

\* Corresponding author

Manuscript received: 29 March, 2025; revised: 12 August 2025; accepted: 3 September, 2025.

Everest Advances in Science and Technology (EAST), Vol. 1, No. 1, 2025

© Everest Engineering College, 2025; all rights reserved.

## 1. Introduction

Nepal, located at the convergence of the Indian and Eurasian tectonic plates, is among the most seismically active regions in the world, ranking 11th globally in terms of earthquake hazard [1]. Historical earthquakes, such as the 1934 Bihar-Nepal earthquake (M8.0) and the 2015 Gorkha earthquake (M7.8), have demonstrated the devastating consequences of seismic events, including significant loss of life, infrastructural damage, and economic disruption. The 2015 Gorkha earthquake alone resulted in over 8,790 fatalities, 22,300 injuries, and an estimated economic loss of \$7 billion, underscoring the urgent need for improved seismic resilience in Nepal's built environment [2].

Commonly used energy dissipating technique to reduce dynamic vibration due to earthquake include shear walls, base isolation systems, tuned mass dampers, and viscous dampers Chopra [3]. Seismic retrofitting through supplementary damping had raised as important strategy for enhancing structural resilience against earthquake. Hankouri et al. [4] investigated the effectiveness of nonlinear viscous dampers (NLVDs) in mitigating seismic responses of multi-degree-of-freedom (MDOF) structures through numerical simulations using Newmark's Beta and Wilson' Theta methods. Their key findings reveal that lower nonlinearity exponents ( $\alpha$ ) and higher damping constants (C) significantly reduce structural displacements, particularly under low peak ground acceleration (PGA) conditions.

Building on this, Kim et al. [5] introduced performance-based design (PBD) procedure for supplemental viscous dampers using the non-iterative capacity spectrum method (CSM) to determine required damping by comparing the demand spectrum with the structure's capacity, achieving displacement error below 10% in both SDOF and MDOF systems. Their study, which distributes dampers proportionally to inter-storey drifts, simplifies the design process such as neglecting higher mode effects. Zhou et al. [6] expanded this work by proposing a practical two-stage design method for retrofitting reinforced concrete (RC) structures with viscous dampers to meet updated seismic codes following the 2008 Wenchuan earthquake. Key findings show that viscous dampers effectively reduce inter-story drifts and story shear forces by approximately 30%; further, they validated through a case study of an RC frame building, demonstrating improved performance under minor, moderate, and major earthquakes. Unlike Kim et al. [5], Zhou's [6] approach does not address higher mode effects explicitly.

Chopra et al. [7] addressed higher mode effects through modal pushover analysis (MPA), combining multiple mode shapes to improve accuracy for mid to high-rise buildings but increased computational complexity, limiting its practicality for rapid assessments. Chopra et al. [8] investigated the seismic response of single-degree-of-freedom (SDF) systems equipped with NLVDs with different damping ratio and non-linearity parameter ( $\alpha$ ), concluding supplementary damping effectively reduces deformation by 60% for damping of 30%. Further, they suggested NLVD achieve comparable response reductions to linear dampers but with significantly lower damper forces.

Experimental investigation carried by Hwang et al. [9] from shaking table tests conducted on two scaled down (1/2.5) three-storey RC building models—one with toggle-brace-mounted viscous dampers and one without—found up to 44% reduction in roof displacement under strong ground motions. Effect of bracing stiffness on damper effectiveness was investigated by Dong et al. [10] and suggested that brace stiffness significantly

impacts system performance—brace stiffness ( $\geq 5 \times$  storey stiffness) enhances damping effectiveness while flexible braces reduce damping efficiency. Drift-based optimization method by Mousavi et al. [11] for determining the optimal placement of damper shows enhanced seismic performance over uniform distribution in high-rise buildings. Simplified performance-based design method over traditional complex method by Ijmulwar et al. [12] showing column forces and base shear decreased by 20–30% resulting 30% damping cost over uniform distributions.

Traditional seismic design in Nepal relies on ductile detailing and shear walls to dissipate energy through inelastic deformations Chaulagain et al. [13]. However, these methods often lead to localized damage, serviceability issues, and increased construction costs due to oversized structural members Gautam et al. [14]. In high seismic zones, such as Kathmandu Valley, conventional approaches may also amplify base shear due to added mass from stiffer elements Chaulagain et al. [15]. Passive energy dissipation systems, particularly fluid viscous dampers (FVDs), offer a promising alternative by enhancing damping ratios without significantly altering structural stiffness Constantinou et al. [16], Symans et al. [17].

Despite their proven efficacy globally, FVDs remain underutilized in Nepal due to a lack of localized studies and absence of codal provisions (e.g., NBC 105:2020). In context of Nepal, Tiwari et al. [18] studied the use of nonlinear fluid viscous dampers (FVDs) in regular RC framed structures and found significant reduction in maximum storey displacement (up to 80% for DBE, 63% for MCE) in 5-storey RC frame buildings with effectiveness decreasing in taller 10 and 15-storey buildings. Their highlight the need for further research on irregular structures.

Current study addresses this gap by evaluating the impact of fluid viscous dampers for vertically irregular buildings subjected to spectrum-compatible ground motions. The findings aim to inform future code revisions and promote the safe implementation of damping technologies in Nepal's diverse building stock.

## 2. Methodology

This study evaluates the effectiveness of NLVDs in enhancing the seismic performance of 10-storey reinforced concrete (RC) buildings with setbacks, exhibiting vertical irregularity. Two models—one without dampers (bare frame) and the other with dampers—were modeled in three-dimensional finite element modelling software SAP2000 v20 (see Figure 1, Figure 2, Figure 3 and Figure 4).

Initially, the building was designed using the Equivalent Lateral Force (ELF) method and Response Spectrum Method for the Design Basis Earthquake (DBE) level as per NBC 105:2020, and all the design checks satisfied the required criteria. The design incorporates beams of dimensions  $600 \times 400$  mm and columns of  $650 \times 600$  mm using M20 grade concrete and Fe415 grade reinforcement. The overall building plan measures  $16 \text{ m} \times 16 \text{ m}$  in the X and Y directions, with a total height of 40 m comprising 10 storeys of 4 m each. Vertical irregularity is introduced in the form of a setback starting from the 5<sup>th</sup> storey, reducing the floor area by 50% in the upper five storeys.

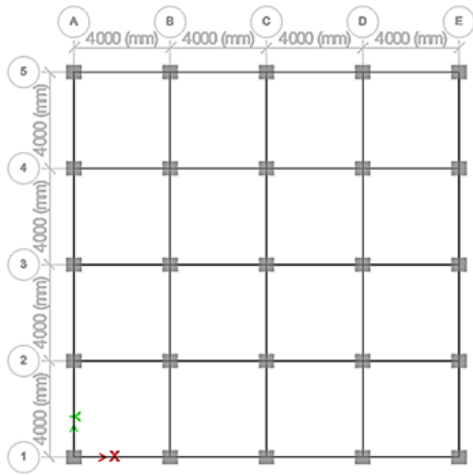


FIGURE 1. Plan of representative building.

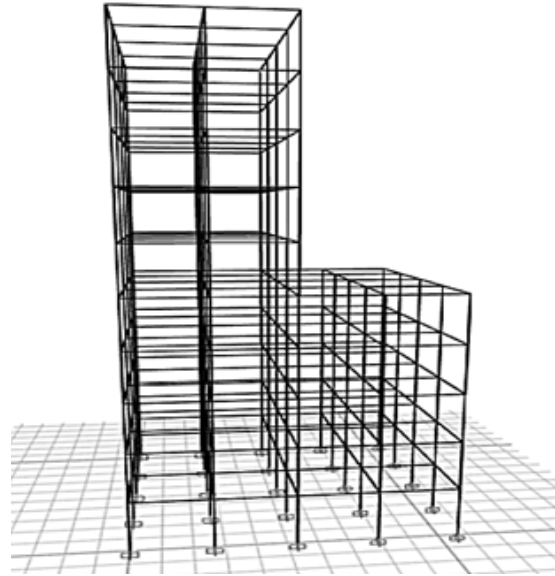


FIGURE 2. 3D Representative building for bare frame.

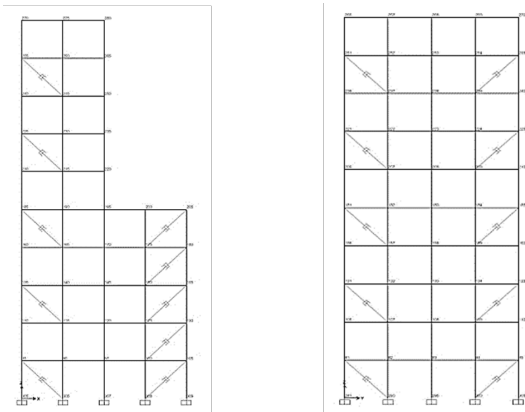


FIGURE 3. Along X-and Y-direction.

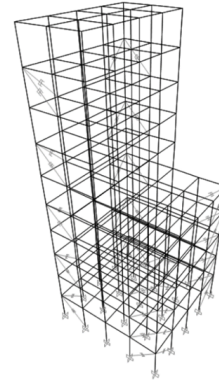


FIGURE 4. 3D representation of building with FVDs.

Nonlinear behavior is incorporated via a lumped plasticity model, where beams are assigned user-defined M3 hinges at offsets of  $0.1L$  and  $0.9L$  from their ends. Columns are assigned automatic P-M2-M3 hinges at similar offsets, in accordance with ASCE 41-13 guidelines. Pushover analysis was performed to obtain the capacity curve, which was then matched with the elastic spectrum for Type D soil as per NBC 105:2020 [19], in Acceleration-Displacement Response Spectrum (ADRS) format to determine the performance point (see Figure 5 and Figure 6).

After that, hinge states at the performance point were evaluated to ensure compliance with the Immediate Occupancy (IO) performance level. In cases where the IO level was exceeded, fluid viscous dampers (FVDs) were strategically placed at storeys exhibiting maximum inter-storey drift. The target damping ratio was determined by iteratively

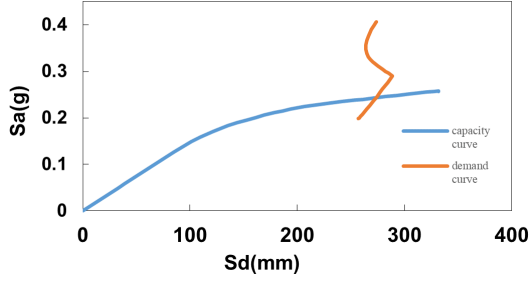


FIGURE 5. Capacity curve and demand curve in X-direction.

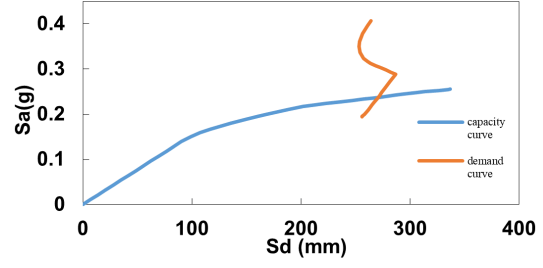


FIGURE 6. Capacity curve and demand curve in Y-direction.

modifying the total damping (inherent + supplementary) in the ADRS procedure, increasing it from the baseline 5% ( $\zeta = 0.05$ ) to higher values (e.g., 0.10, 0.15, 0.20), and observing the shift in the demand spectrum and the resulting performance point. Through this iterative process, it was found that a supplementary damping ratio of approximately 30% was required to achieve the IO performance level. The total supplementary damping coefficient was calculated as per the method proposed by Mousavi et al. [11], using Equation (1):

$$C_A = \frac{(\zeta^* - \zeta) T K}{\pi} \quad (1)$$

where  $C_A$  is the total supplementary damping coefficient (N-sec/mm),  $\zeta^*$  is the required (supplementary) damping ratio,  $\zeta$  is the inherent damping ratio,  $T$  is the fundamental time period of the structure (sec), and  $K$  is the total lateral stiffness of the structure (kN/mm).

The linear properties of FVDs were then converted into nonlinear damper properties following the procedure suggested by Canney et al. [20]. The FVDs were modeled as two-noded nonlinear link elements, characterized by a stiffness of 500 kN/mm, damping coefficients of 1250 N-sec/mm and 1500 N-sec/mm, and a damping exponent  $\alpha = 0.3$ . The two damping coefficients correspond to dampers with different energy dissipation capacities, strategically placed at different storey levels based on the inter-storey drift ratios identified from the pushover analysis. By introducing velocity-dependent dampers, the structural damping increased, enabling enhanced energy dissipation through forces proportional to relative velocity. This mechanism reduces vibration amplitudes and limits inelastic deformations during seismic events. While the pushover procedure for determining target damping is primarily governed by the fundamental mode, this limitation was mitigated by conducting nonlinear time history analysis (NLTHA) using seven spectrum-compatible ground motions matched to NBC 105:2020.

Seven ground motion records (refer Table 1) were selected and matched to the NBC 105:2020 elastic response spectrum for Type D soil, corresponding to a 10% probability of exceedance in 50 years (DBE) for use in nonlinear time history analysis (NLTHA). Figure 7 represents the mean matched response spectrum for the selected ground motions.

TABLE 1. Selected Ground Motions for Study

S.N.	Earthquake Name	Event Day	PGA (g)	Magnitude (M)	Recording Station
1	Gorkha Earthquake	4/25/2015	0.25	7.8	Kanti Path, Kathmandu
2	Imperial Valley	10/15/1979	0.317	6.6	USGS STATION 5115
3	Chi-Chi	9/20/1999	0.361	7.62	TCU045
4	Kocaeli	8/17/1999	0.349	7.51	Yarimca
5	Landers	6/28/1992	0.78	7.28	See Station 24
6	Loma Prieta	10/18/1989	0.367	6.93	CDMG Station 47381
7	Kobe	1/16/1995	0.311	6.9	Kakogawa

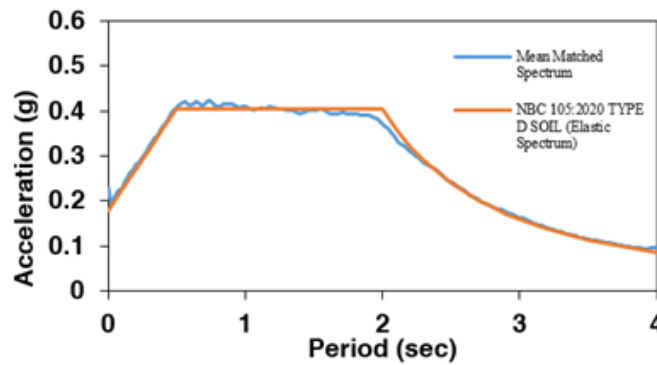


FIGURE 7. Mean matched spectrum matched with NBC105:2020 elastic spectrum at DBE level earthquake.

The analyses were conducted using the Direct Integration method in SAP2000 to capture the full dynamic response of the structure. Maximum storey displacements for each model were evaluated in both X and Y directions, along with hinge states, to confirm compliance with the Immediate Occupancy (IO) performance level as defined by ASCE 41-13 [21]. The IO performance level ensures that the structure sustains minimal damage during a seismic event, allowing for immediate reoccupation post-earthquake.

### 3. Maximum Storey Displacement

The outcomes from the nonlinear time history analysis (NLTHA) were plotted to compare the maximum displacement at each storey for both models: the bare frame and the frame equipped with fluid viscous dampers (FVDs), under multiple ground motions. Table 2 and Table 3 present the maximum storey displacements for different ground motions in the X and Y directions, respectively, for the bare frame model. Figure 8 and Figure 9 provide a clear visual comparison of displacement profiles for both structural configurations.

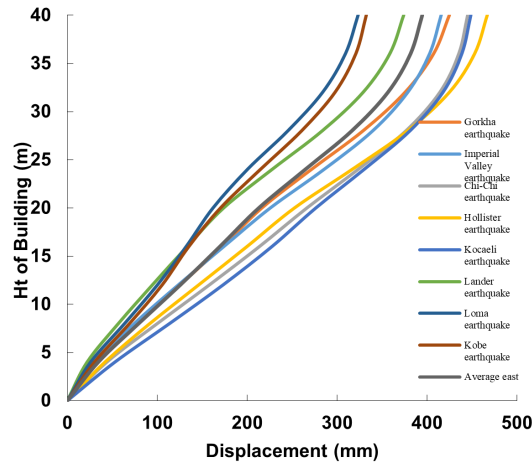


FIGURE 8. Maximum storey displacement of bare frame along X direction.

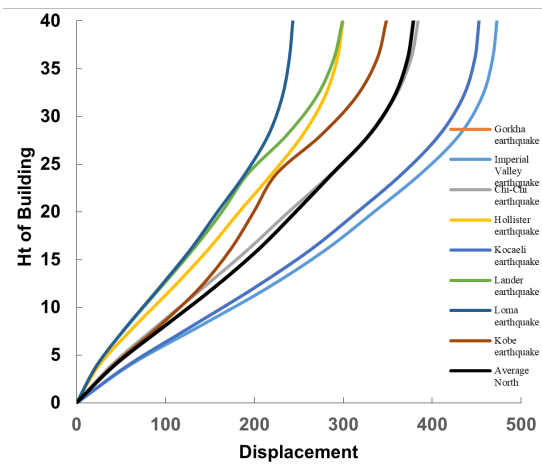


FIGURE 9. Maximum storey displacement of bare frame along Y-direction.

TABLE 2. Maximum storey displacement for bare frame along X direction (mm)

Storey	Gorkha	Imperial - Valley	ChiChi	Kocaeli	Landers	Loma	Kobe
Tenth	425	416	445	449	374	323	332
Ninth	407	403	435	439	358	309	321
Eighth	375	379	414	418	329	284	298
Seventh	329	340	377	381	283	245	261
Sixth	271	286	323	330	228	200	215
Fifth	216	226	267	276	174	162	170
Fourth	172	174	214	228	133	132	135
Third	125	123	158	173	94	100	105
Second	78	74	100	114	57	64	69
First	34	32	44	53	22	26	30
G.F.	0	0	0	0	0	0	0

The integration of fluid viscous dampers (FVDs) into the structural frame significantly enhanced the seismic performance, as evidenced by the maximum storey displacement data presented in the following tables. Analysis of the displacement results revealed that the average maximum displacement for the bare frame, which reached up to 394 mm, was reduced by approximately 60–70% with the incorporation of FVDs. Table 4 and Table 5 present the maximum storey displacements for different ground motions in the X and Y directions, respectively, for the frame equipped with FVDs. Figure 11 and Figure 10 provide clear visual representations of these displacements.

TABLE 3. Maximum Storey Displacement for Bare Frame along Y Direction (mm)

Storey	Gorkha	Imperial-Valley	Chi-Chi	Kocaeli	Landers	Loma	Kobe
Tenth	453	473	384	453	299	243	349
Ninth	448	468	376	448	289	239	338
Eighth	435	456	358	435	270	231	314
Seventh	408	430	329	408	236	216	275
Sixth	366	387	287	366	193	190	225
Fifth	316	334	239	316	163	158	199
Fourth	263	280	192	263	130	128	173
Third	199	214	142	199	94	92	138
Second	129	138	90	129	57	56	92
First	59	60	40	59	23	23	42
G.F.	0	0	0	0	0	0	0

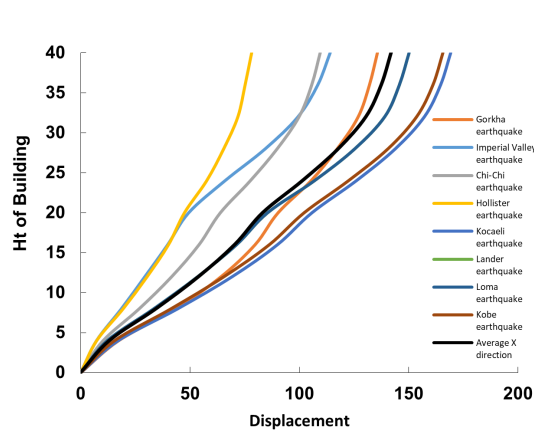


FIGURE 10. Maximum storey displacement of frame with FVDs along X direction.

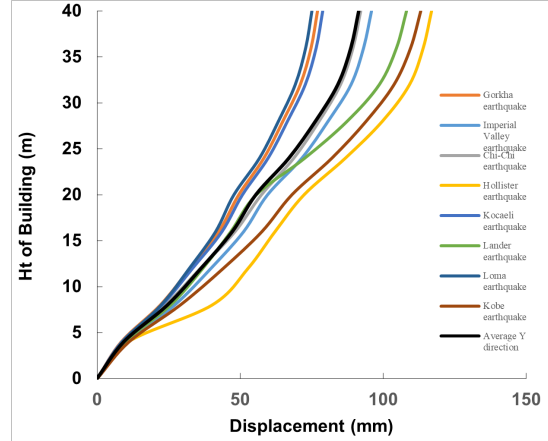


FIGURE 11. Maximum storey displacement of frame with FVDs along Y direction.

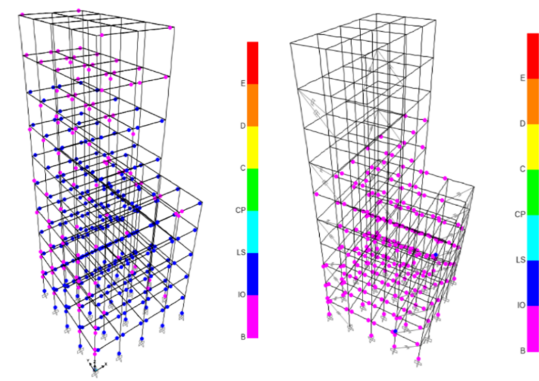


FIGURE 12. Hinge mechanism for Gorkha earthquake.

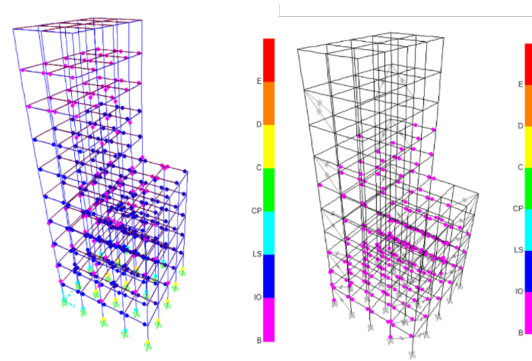


FIGURE 13. Hinge mechanism for Chi-Chi earthquake.

TABLE 4. Maximum Displacement for Frame with FVDs along X Direction (mm)

Storey	Gorkha	Imperial-Valley	Chi-Chi	Kocaeli	Landers	Loma	Kobe
Tenth	136	114	110	169	150	149	166
Ninth	132	108	106	165	146	144	161
Eighth	127	99	100	157	139	137	154
Seventh	117	84	90	144	125	123	140
Sixth	105	66	78	126	107	106	122
Fifth	90	49	64	106	85	86	102
Fourth	80	40	54	90	71	72	86
Third	64	29	42	69	53	54	65
Second	43	19	27	44	33	34	41
First	17	7	10	17	12	13	15
G.F.	0	0	0	0	0	0	0

TABLE 5. Maximum Displacement for Frame with FVDs along Y Direction (mm)

Storey	Gorkha	Imperial-Valley	Chi-Chi	Kocaeli	Landers	Loma	Kobe
Tenth	77	96	92	79	108	75	113
Ninth	75	93	90	77	105	73	110
Eighth	71	89	85	73	99	69	104
Seventh	65	81	78	67	87	63	94
Sixth	58	72	69	60	73	57	82
Fifth	49	60	57	51	56	48	68
Fourth	42	51	48	44	47	41	58
Third	32	40	36	33	37	32	44
Second	22	27	24	23	26	22	29
First	8	10	9	9	10	9	11
G.F.	0	0	0	0	0	0	0

TABLE 6. Hinge State for Bare Frame and Frame with FVDs for Different Ground Motions

Storey	Gorkha Earthquake		Chi-Chi Earthquake			
	Bare Frame B-IO	Frame with FVDs IO-LS	Bare Frame B-IO	Bare Frame IO-LS	Bare Frame LS-CP	Frame with FVDs B-IO
G.F.	3	22	0	17	8	7
First	13	43	25	40	0	46
Second	10	40	10	44	0	42
Third	6	40	10	46	0	40
Fourth	8	40	9	45	0	20
Fifth	22	33	15	41	0	15
Sixth	0	20	6	20	0	18
Seventh	10	20	10	20	0	8
Eighth	14	14	28	0	0	0
Ninth	23	0	19	0	0	0
Tenth	4	0	0	0	0	0

#### 4. Plastic Hinge Mechanism

The results of hinge formation after NLTHA, were evaluated to compare seismic performance of a) bare frame model without FVDs and b) a frame incorporating FVDs against different ground motion. Table 6 represents the hinge state in tabulated form representing different state of performance level for bare frame and frame with FVDs for different

TABLE 7. Hinge State for Bare Frame and Frame with FVDs for Kobe and Loma Earthquakes






Storey	Kobe Earthquake		Loma Earthquake			
	Bare Frame B-IO	Frame with FVDs IO-LS	Bare Frame B-IO	Bare Frame IO-LS	Bare Frame LS-CP	Frame with FVDs B-IO
G.F.	10	15	24	20	5	25
First	7	13	55	38	10	57
Second	9	40	50	13	38	50
Third	46	0	42	35	11	42
Fourth	36	7	40	42	4	40
Fifth	35	19	43	38	20	36
Sixth	0	20	20	0	20	20
Seventh	0	20	11	6	20	20
Eighth	23	0	0	30	0	7
Ninth	20	0	0	20	0	0
Tenth	0	0	0	0	0	0

TABLE 8. Hinge State for Bare Frame and Frame with FVDs for Imperial Valley and Kocaeli Earthquakes

Storey	Imperial Valley			Kocaeli Earthquake				
	Bare Frame B-IO	Frame with FVDs IO-LS	Frame with FVDs B-IO	Bare Frame B-IO	Bare Frame IO-LS	Bare Frame LS-CP	Bare Frame CP-C	Frame with FVDs B-IO
G.F.	23	25	7	0	0	12	0	21
First	8	34	22	23	40	0	0	51
Second	7	40	34	9	47	0	0	47
Third	41	18	11	46	0	0	0	42
Fourth	5	45	11	12	44	0	0	40
Fifth	19	37	25	12	33	0	0	33
Sixth	6	20	20	0	20	0	0	20
Seventh	10	20	20	6	20	0	0	20
Eighth	23	0	14	24	0	0	0	4
Ninth	20	0	0	20	0	0	0	0
Tenth	0	0	0	0	0	0	0	0

Landers Earthquake			
Storey	Bare Frame		Frame with FVDS
	B-IO	IO-LS	B-IO
G.F.	20	5	25
First	58	3	55
Second	19	34	44
Third	14	40	40
Fourth	13	38	42
Fifth	33	30	36
Sixth	0	20	20
Seventh	9	20	20
Eighth	16	17	7
Ninth	23	0	0
Tenth	14	0	0

TABLE 9. Color code for Different Performance Level.

Performance Level	B-IO	IO-LS	LS-CP	CP-C	C-D
Color Code					

ground motions. Refer Figure 12 to Figure 18 for clear visual representation of hinge states.

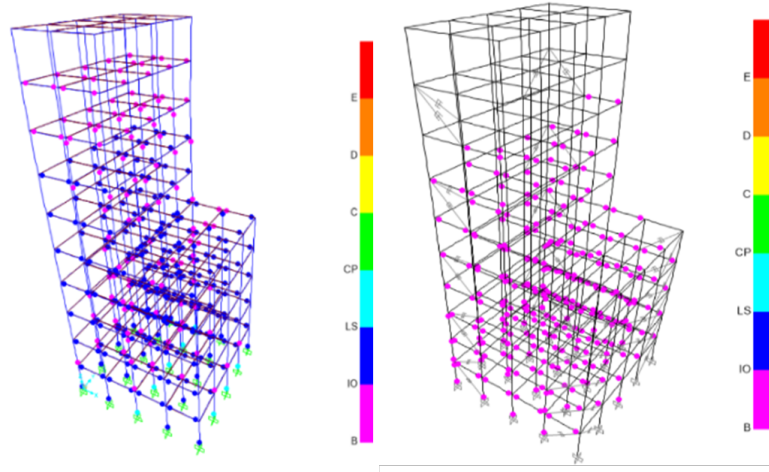


FIGURE 18. Hinge mechanism for Kocaeli earthquake.

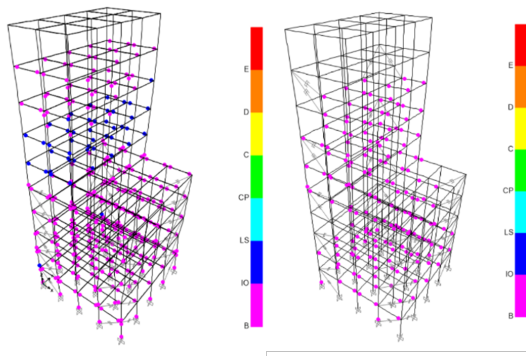


FIGURE 14. Hinge mechanism for Imperial Valley earthquake.

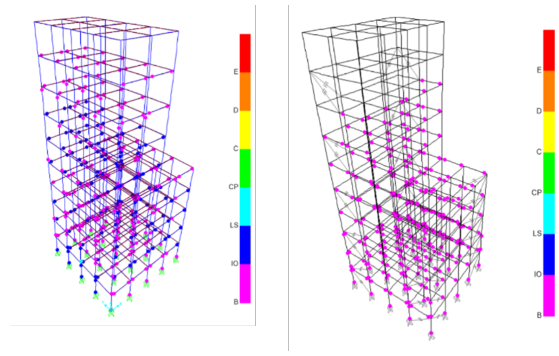


FIGURE 15. Hinge mechanism for Kobe Valley earthquake.

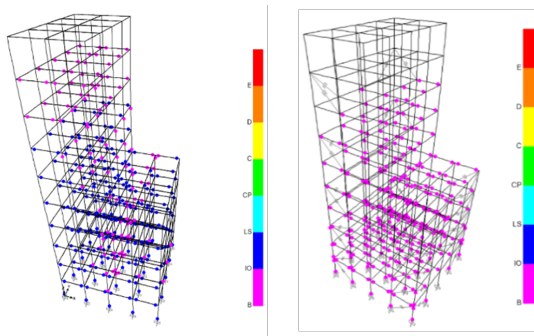


FIGURE 16. Hinge mechanism for Loma Prieta earthquake.

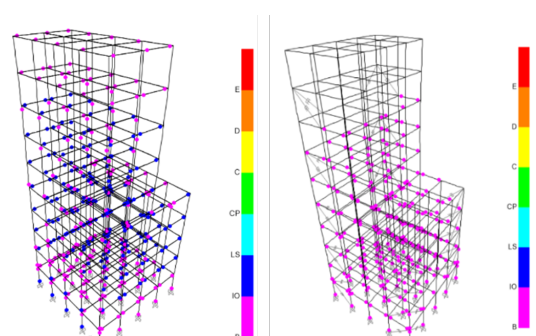


FIGURE 17. Hinge mechanism for Lander earthquake.

## 5. Conclusion

This study demonstrates the effectiveness of NLVDs in enhancing the seismic performance of a vertically irregular 10-storey RC building with setback. By incorporating performance-based design principles and conducting both pushover and NLTHA, it was observed that the addition of FVDs significantly reduced maximum storey displacements and controlled hinge states within the IO performance level. The strategic placement of FVDs at stories with maximum inter-storey drift proved crucial in improving structural response. These findings highlight the practical applicability of FVDs in Nepalese seismic design, especially for irregular buildings, and support the need for their consideration in future updates to the national building code. However, effectiveness of FVDs with an increase in building height, as well as challenges in addressing complex plan irregularities, which may require further investigation.

## References

- [1] UNDP, *Reducing disaster risk: a challenge for development, a global report*. New York: United Nations Development Programme, 2004. [Online]. Available: <https://www.undp.org/publications/reducing-disaster-risk-challenge-development>
- [2] S. N. Sapkota, L. Bollinger, and F. Perrier, "Fatality rates of the  $M_w$  8.2, 1934, Bihar–Nepal earthquake and comparison with the April 2015 Gorkha earthquake," *Earth Planets Space*, vol. 68, no. 1, Dec. 2016, doi: 10.1186/s40623-016-0416-2.
- [3] A. K. Chopra, *Dynamics of Structures: Theory and Applications to Earthquake Engineering*, 4th ed. Pearson, 2012.
- [4] Y. El Hankouri and A. El Ghoulbzouri, "A Numerical Investigation of the Impact of Non-linear Viscous Damping on Structural Response to Seismic Excitation," *Iran J Sci Technol Trans Civ Eng*, Feb. 2025, doi: 10.1007/s40996-025-01743-3.
- [5] J. Kim, H. Choi, and K.-W. Min, "Performance-based design of added viscous dampers using capacity spectrum method," *J. Earthquake Eng.*, vol. 7, no. 1, pp. 1–24, Jan. 2003, doi: 10.1080/13632460309350439.
- [6] Y. Zhou, X. Lu, D. Weng, and R. Zhang, "A practical design method for reinforced concrete structures with viscous dampers," *Eng. Struct.*, vol. 39, pp. 187–198, Jun. 2012, doi: 10.1016/j.engstruct.2012.02.014.
- [7] A. K. Chopra and R. K. Goel, "A modal pushover analysis procedure for estimating seismic demands for buildings," *Earthq. Eng. Struct. Dyn.*, vol. 31, no. 3, pp. 561–582, Mar. 2002, doi: 10.1002/eqe.144.
- [8] W. Lin and A. K. Chopra, "Earthquake response of elastic SDF systems with non-linear fluid viscous dampers," *Earthq. Eng. Struct. Dyn.*, vol. 31, no. 9, pp. 1623–1642, Sep. 2002, doi: 10.1002/eqe.179.
- [9] J.-S. Hwang, C.-H. Tsai, S.-J. Wang, and Y.-N. Huang, "Experimental study of RC building structures with supplemental viscous dampers and lightly reinforced walls," *Eng. Struct.*, vol. 28, no. 13, pp. 1816–1824, Nov. 2006, doi: 10.1016/j.engstruct.2006.03.012.
- [10] B. Dong, R. Sause, and J. M. Ricles, "Modeling of nonlinear viscous damper response for analysis and design of earthquake-resistant building structures," *Bull. Earthquake Eng.*, vol. 20, no. 3, pp. 1841–1864, Feb. 2022, doi: 10.1007/s10518-021-01306-7.
- [11] S. A. Mousavi and A. K. Ghorbani-Tanha, "Erratum to: Optimum placement and characteristics of velocity-dependent dampers under seismic excitation," *Earthq. Eng. Eng. Vib.*, vol. 11, no. 4, pp. 603–603, Dec. 2012, doi: 10.1007/s11803-012-0145-x.
- [12] S. S. Ijmulwar and S. K. Patro, "Seismic design of reinforced concrete buildings equipped with viscous dampers using simplified performance-based approach," *Structures*, vol. 61, p. 106020, Mar. 2024, doi: 10.1016/j.istruc.2024.106020.
- [13] D. Gautam and H. Chaulagain, "Structural performance and associated lessons to be learned from world earthquakes in Nepal after 25 April 2015 (MW 7.8) Gorkha earthquake," *Eng. Fail. Anal.*, vol. 68, pp. 222–243, Oct. 2016, doi: 10.1016/j.engfailanal.2016.06.002.
- [14] D. Gautam, R. Adhikari, and R. Rupakhety, "Seismic fragility of structural and non-structural elements of Nepali RC buildings," *Eng. Struct.*, vol. 232, p. 111879, Apr. 2021, doi: 10.1016/j.engstruct.2021.111879.

- [15] H. Chaulagain, H. Rodrigues, J. Jara, E. Spacone, and H. Varum, "Seismic response of current RC buildings in Nepal: A comparative analysis of different design/construction," *Eng. Struct.*, vol. 49, pp. 284–294, Apr. 2013, doi: 10.1016/j.engstruct.2012.10.036.
- [16] M. C. Constantinou, T. T. Soong, and G. F. Dargush, *Passive energy dissipation systems for structural design and retrofit*. Buffalo, NY: Multidisciplinary Center for Earthquake Engineering Research, 1998.
- [17] M. D. Symans *et al.*, "Energy Dissipation Systems for Seismic Applications: Current Practice and Recent Developments," *J. Struct. Eng.*, vol. 134, no. 1, pp. 3–21, Jan. 2008, doi: 10.1061/(ASCE)0733-9445(2008)134:1(3).
- [18] P. Tiwari, P. Badal, and R. Suwal, "Effectiveness of fluid viscous dampers in the seismic performance enhancement of RC buildings," *Asian J. Civ. Eng.*, vol. 24, no. 1, pp. 309–318, Jan. 2023, doi: 10.1007/s42107-022-00504-1.
- [19] Government of Nepal, *NBC 105:2020, Seismic design of buildings in Nepal*.
- [20] Taylor Devices Inc., "Non-Ductile Concrete Moment Frame Retrofit Design Guide." [Online]. Available: [https://www.taylordevices.com/wp-content/uploads/Taylor-Devices\\_Non-Ductile-Concrete-Moment-Frame-Retrofit-Design-Guide.pdf](https://www.taylordevices.com/wp-content/uploads/Taylor-Devices_Non-Ductile-Concrete-Moment-Frame-Retrofit-Design-Guide.pdf)
- [21] American Society of Civil Engineers, *Seismic Evaluation and Retrofit of Existing Buildings*, 41st ed. Reston, VA: ASCE, 2014, doi: 10.1061/9780784412855.